Properties of HERG Channels Stably Expressed in HEK 293 Cells Studied at Physiological Temperature

Zhengfeng Zhou, Qiuming Gong, Bin Ye, Zheng Fan, Jonathan C. Makielski, Gail A. Robertson, and Craig T. January

Departments of Medicine (Cardiology) and Physiology, University of Wisconsin, Madison, Wisconsin 53792 USA

ABSTRACT We have established stably transfected HEK 293 cell lines expressing high levels of functional human ether-a go-go-related gene (HERG) channels. We used these cells to study biochemical characteristics of HERG protein, and to study electrophysiological and pharmacological properties of HERG channel current at 35°C. HERG-transfected cells expressed an mRNA band at 4.0 kb. Western blot analysis showed two protein bands (155 and 135 kDa) slightly larger than the predicted molecular mass (127 kDa). Treatment with *N*-glycosidase F converted both bands to smaller molecular mass, suggesting that both are glycosylated, but at different levels. HERG current activated at voltages positive to −50 mV, maximum current was reached with depolarizing steps to −10 mV, and the current amplitude declined at more positive voltages, similar to HERG channel current expressed in other heterologous systems. Current density at 35°C, compared with 23°C, was increased by more than twofold to a maximum of 53.4 ± 6.5 pA/pF. Activation, inactivation, recovery from inactivation, and deactivation kinetics were rapid at 35°C, and more closely resemble values reported for the rapidly activating delayed rectifier K^+ current (I_{Kr}) at physiological temperatures. HERG channels were highly selective for K^+. When we used an action potential clamp technique, HERG current activation began shortly after the upstroke of the action potential waveform. HERG current increased during repolarization to reach a maximum amplitude during phases 2 and 3 of the cardiac action potential. HERG contributed current throughout the return of the membrane to the resting potential, and deactivation of HERG current could participate in phase 4 depolarization. HERG current was blocked by low concentrations of E-4031 (IC_{50} 7.7 nM), a value close to that reported for I_{Kr} in native cardiac myocytes. Our data support the postulate that HERG encodes a major constituent of I_{Kr} and suggest that at physiological temperatures HERG contributes current throughout most of the action potential and into the postrepolarization period.

INTRODUCTION

Delayed rectifier potassium current (I_K) plays a critical role in the control of action potential repolarization in many cell types. In mammalian and human cardiac myocytes, I_K is composed of at least two distinct currents, I_{Kr} and I_{Ks} (Li et al., 1996b; see also Sanguinetti and Jurkiewicz, 1990), and genes for both I_{Kr} and I_{Ks} have been identified (Warmke and Ganetzky, 1994; Sanguinetti et al., 1996b). A third ultrarapidly activating delayed rectifier current, I_{Kur}, has also been identified in atrial tissue (Wang et al., 1993; Li et al., 1996a).

Human ether-a go-go-related gene (HERG) was originally cloned from human hippocampus by Warmke and Ganetzky (1994), and it is strongly expressed in the heart (Curran et al., 1995). When studied in *Xenopus* oocytes, or transiently expressed in HEK 293 cells, HERG encodes a K^+ channel with many characteristics of I_{Kr} (Sanguinetti et al., 1995; Trudeau et al., 1995; Snyders and Chaudhary, 1996). HERG is a target for block by many drugs (Trudeau et al., 1995; Snyders and Chaudhary, 1996; Spector et al., 1996a; January and Zhou, 1997; Mohammad et al., 1997), and defects in HERG have been shown in multiple types of chromosome 7-linked inherited long QT syndrome (Curran et al., 1995; Tanaka et al., 1997). In the present study, we have established stably transfected cell lines expressing high levels of functional HERG channels. We studied biochemical characteristics of the HERG protein, and electrophysiological and pharmacological properties of these HERG channels at physiological temperature. We also used an action potential clamp technique to study the physiological role HERG current may play during a cardiac ventricular action potential. Portions of this work have appeared in abstract form (Zhou et al., 1997).

Received for publication 13 June 1997 and in final form 29 September 1997.

Address reprint requests to Dr. Craig T. January or Dr. Zhengfeng Zhou, Department of Medicine (Cardiology), University of Wisconsin Hospital and Clinics, Room H6/352, 600 Highland Ave., Madison, WI 53792. Tel.: 608-262-5291; Fax: 608-263-0405; E-mail: ctj@medicine.wisc.edu.

0006-3495/98/01/230/12 $2.00

MATERIALS AND METHODS

DNA constructs and stable transfection of HEK 293 cells

HERG cDNA (Trudeau et al., 1995, 1996) was subcloned into *Bam*HI/*Eco*RI sites of the pCDNA3 vector (Invitrogen). This vector contains a CMV promoter and a SV40 promoter, which drive the expression of the inserted cDNA (HERG) and neomycin-resistant gene, respectively. The HEK 293 cells were transfected with this construct by a calcium phosphate precipitate method (Gibco) or a lipofectamine method (Gibco). After selection in 800 μg/ml geneticin (G418; Gibco) for 15–20 days, single colonies were picked with cloning cylinders and tested for HERG current. The stably transfected cells were cultured in minimum essential medium (MEM) supplemented with 10% fetal bovine serum and 400 μg/ml G418.

For electrophysiological study, the cells were harvested from the culture dish by trypsinization, washed twice with standard MEM medium, and

stored in this medium at room temperature for later use. Cells were studied within 8 h of harvest.

Northern blot analysis

Total RNA was prepared with RNAzol (Tel-Test, Friendwood, TX) according to the manufacturer's instructions. RNA samples (15 μg/lane) were denatured with formamide and formaldehyde and subjected to electrophoresis in 1% agarose gel. The gel was stained with ethidium bromide to confirm that equivalent amounts of RNA were loaded on each lane. The RNAs were transferred to a nitrocellulose filter. The filter was prehybridized for 4 h in a solution containing 50% formamide, 5× Denhardt's solution (Maniatis et al., 1987), 0.25 mg/ml of denatured salmon sperm DNA, 1.0% sodium dodecyl sulfate (SDS), 1.0 M NaCl, 10 mM Na_2HPO_4, and 0.1% tetrasodium pyrophosphate. Hybridization was allowed to take place at 42°C overnight in a fresh mixture of the same solution, to which ^{32}P-labeled HERG cDNA had been added. After hybridization the filter was washed three times (30 min each time) in 0.2× sodium chloride/sodium citrate and 0.5% SDS at 65°C, and exposed to Kodak BMR film with an intensifying screen for 48 h.

Western blot analysis

Parallel plates of similarly confluent cultures were used to isolate crude membrane fractions. All steps were performed at 4°C. Briefly, the cells from 100-mm plates were rinsed with PBS and scraped off into a 2-ml solution of 200 mM NaCl, 33 mM NaF, 10 mM EDTA, 50 mM HEPES (pH 7.4 with NaOH) plus a protease inhibitor cocktail (100 μM phenylmethylsulfonyl fluoride, 1 μg/ml pepstatin A, 1 μg/ml of leupeptin, 4 μl/ml of aprotinin). The cells were homogenized and spun at 500 × *g* for 10 min. The membrane fractions were pelleted from the low-speed supernatants by centrifugation at 60,000 r.p.m. in a TLA 100.1 rotor (Beckman) for 1 h at 4°C, and resuspended in 50 mM Tris-HCl, 15 mM β-mercaptoethanol, and 1% SDS. The membrane proteins (50 μg sample) were boiled in sample buffer (0.12 M Tris-HCl, pH 6.8, 2% SDS, 2% mercaptoethanol, 20% glycerol, and 0.001% bromphenol blue), and electrophoresed on a 7.5% polyacrylamide SDS gel (Laemmli, 1970). The membrane proteins were then electrophoretically transferred onto nitrocellulose filter (S&S) by using a trans-blot system (Bio-Rad). After transfer, the filters were blocked with 5% nonfat dry milk and 0.2% Tween 20 in PBS (Western buffer) for 1 h. The filters were then incubated with purified rabbit polyclonal anti-HERG antibodies (a gift from Drs. A. Pond and J. Nerbonne, Department of Pharmacology and Molecular Biology, Washington University, St. Louis, MO; see Pond and Nerbonne, 1996) at a 1:500 dilution at room temperature overnight. One antibody recognized the C-terminus (residues 1145–1159, LTSQPLHRHGSDPGS), and the other antibody recognized a region close to the N-terminus (residues 174–188, TARESSVRSGGAGGA). The filters were then washed with PBS and incubated with horseradish peroxidase-conjugated donkey anti-rabbit immunoglobulin diluted 1:1000 in Western buffer for 2 h at room temperature. After washing with PBS, bound antibodies were detected with the ECL detection kit (Amersham). The light emission produced was detected by autoradiography.

For *N*-glycosidase F treatment, the cell membrane fractions were dissolved in 50 mM sodium phosphate buffer (pH 7.2) containing 20 mM EDTA, 1% β-mercaptoethanol, and 1% SDS by boiling for 2 min; additional buffer was added to dilute SDS to 0.1%. NP-40 was added to a final concentration of 1%, followed by addition of 4 units of *N*-glycosidase F for 20 μg membrane proteins. The mixture was then incubated at 37°C for 17 h. The reaction was stopped by adding sample buffer and boiling for 2 min.

Patch-clamp recording techniques

Cells used for electrophysiological study were transferred to a small cell bath mounted on the stage of an inverted microscope (Diaphot, Nikon), and were superfused with HEPES-buffered Tyrode solution containing (in mM) 137 NaCl, 4 KCl, 1.8 $CaCl_2$, 1 $MgCl_2$, 10 glucose, and 10 HEPES (pH 7.4 with NaOH). In a few experiments, KCl was 2 or 10 mM. Solution exchange within the cell bath, as assessed by changes in junction potential with washing in different solutions, was estimated to be complete in ~1.5 min. Membrane currents were recorded in a whole-cell configuration using suction pipettes (Hamill et al., 1981), and leak compensation was not used. The pipette had an inner diameter of 1–1.5 μm, and when filled with the internal pipette solution had a resistance of 2–4 MΩ. The internal pipette solution contained (in mM) 130 KCl, 1 $MgCl_2$, 5 EGTA, 5 MgATP, 10 HEPES (pH 7.2 with KOH). An Axopatch-1D patch-clamp amplifier was used to record membrane currents. Computer software (pCLAMP; Axon Instruments) was used to generate voltage clamp protocols, acquire data, and analyze current traces. The data were stored on a computer hard disc for later analysis. Most experiments were performed at a temperature of 35 ± 1°C, which was maintained with a TC^2 temperature controller (Cell Micro Controls, Virginia Beach, VA). In a few experiments data initially were obtained at 23 ± 1°C, and then the experiment was repeated at 35 ± 1°C in the same cell to permit direct comparison of the effect of temperature. Under these conditions, the temperature change was complete in <30 s. E-4031 was obtained as a gift from Eisai Ltd. (Ibaraki, Japan).

Statistical treatment

Data are given as mean ± standard error of the mean. In cells studied at both 23°C and 35°C, statistical comparison of temperature-dependent effects was made using a paired *t*-test. Curve fitting was done using a nonlinear least-squares regression analysis (pCLAMP, Axon Instruments; Sigmaplot, Jandel Scientific). Cell capacitance was calculated using a voltage ramp function.

RESULTS

More than 10 G-418 resistant cell lines were isolated and tested for the expression of HERG current. Two high current density cell lines (one with each transfection technique) were used for the experiments reported here, with the two cell lines giving similar results. After subcloning, these cell lines expressed HERG current for more than 30 passages over time periods exceeding 6 months.

Northern and Western blot analysis of HERG-transfected cells

Northern blot analysis for total RNA isolated from HERG-transfected cells and control untransfected HEK 293 cells is shown in Fig. 1. HERG-transfected cells exhibited an mRNA band at 4.0 kb, which is the predicted size from HERG cDNA. This mRNA band was not present in untransfected HEK 293 cells.

Western blot analysis of membrane proteins in HERG stably transfected and control untransfected HEK 293 cells is shown in Fig. 2. Antibodies directed against the carboxy terminus (anti-C) and amino terminus (anti-N) were used to probe for HERG protein. As shown in Fig. 2, *A* and *B* (*lane 2*), the anti-N and anti-C antibodies recognize two bands of HERG proteins in transfected cells, an upper broad band with an apparent molecular mass of ~155 kDa and a lower band with an apparent molecular mass of ~135 kDa. Nei-

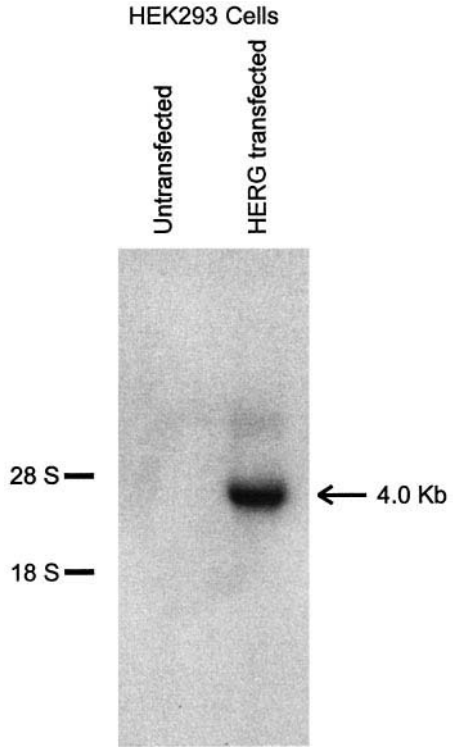

FIGURE 1 Northern blot analysis of mRNA from HEK 293 cells stably transfected with HERG. The ^{32}P-labeled HERG cDNA probe was hybridized to total RNA from HERG-transfected cells and untransfected cells as indicated (15 μg/lane). Size makers are 18S and 28S ribosomal RNA. In HERG-transfected cells there is a 4.0-kb mRNA band.

ther band was present in untransfected HEK 293 cells (Fig. 2, *A* and *B*, *lane 1*).

To test whether the two HERG protein bands result from glycosylation of the channel, we used *N*-glycosidase F to remove N-linked glycosylation of the HERG channel protein. Treatment of the membrane protein with *N*-glycosidase F converted the 155-kDa protein band to a 140-kDa form (Fig. 2 *C*). Treatment with *N*-glycosidase F also shifted the 135-kDa protein band downward by 2–3 kDa. These results suggest that both HERG protein bands undergo *N*-glycosylation. A possibility is that the 155-kDa protein is the fully glycosylated form of HERG channels, whereas the 135-kDa protein is a core-glycosylated form of HERG channels, similar to Shaker K channel proteins (Santacruz-Toloza et al., 1994).

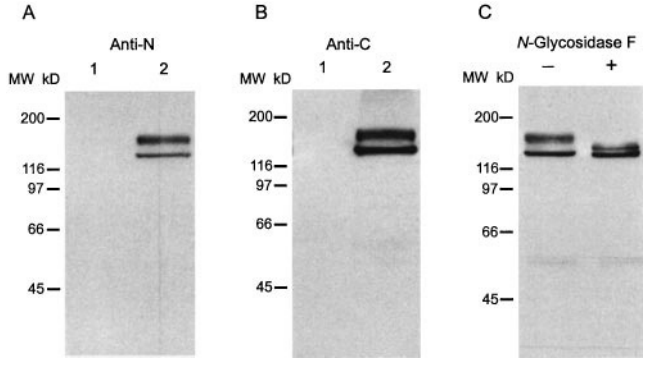

FIGURE 2 Western blot analysis of the expression of HERG channel protein in stably transfected HEK 293 cells. Forty micrograms of crude membrane protein in 50 μl was diluted with 6× sample buffer and separated by SDS-polyacrylanide gel electrophoresis in 7.5% acrylamide gel. Antibodies were detected by chemiluminescence as described in Materials and Methods. (*A* and *B*) Anti-C and anti-N antibody, respectively. Lanes 1 and 2 show results with untransfected cells and cells stably transfected with the cDNA encoding HERG, respectively. (*C*) Data for control conditions (−) and after treatment with *N*-glycosidase F (+).

Electrophysiological properties of HERG current in stably transfected cells

Previous reports using oocyte expression and transient transfection techniques to study HERG current were performed at room temperature. Because the properties of HERG at 35°C are likely to be more representative of native current under physiological conditions, most studies reported here were carried out at 35°C. Some studies were also performed at 23°C to permit the comparison of temperature-dependent effects (see below).

Fig. 3 shows voltage-dependent properties of HERG current at 35°C. Fig. 3 *A* shows original current records obtained from a HERG-transfected cell. The cell was clamped at a holding potential of −80 mV and depolarized to voltages between −60 and 50 mV for 4 s to activate HERG current. The cell was then clamped to −50 mV for 5 s to record a tail current. As shown in the upper set of current traces, during depolarizing steps, an outward current was activated at voltages positive to −50 mV, and the current amplitude was increased to reach a maximum at −10 mV. With further depolarization, the current amplitude decreased progressively. Fig. 3 *B* shows the *I-V* plot of HERG current amplitude at the end of the depolarizing step (circles, $n = 13$ cells). It shows that maximum outward current was present with voltage steps to −10 mV, and at more positive voltages there was a steep negative slope conductance. This property of inward rectification of HERG has been attributed to voltage-dependent channel inactivation (Sanguinetti et al., 1995; Trudeau et al., 1995; Smith et al., 1996; Spector et al., 1996b). Tail current amplitude, normalized to the maximum tail current amplitude, was used to construct the activation curve shown in Fig. 3 *C* ($n = 8$ cells). The activation curve shows that the threshold voltage for HERG current activation is close to −50 mV and that it is fully activated with voltage steps to 0 mV. When fit as a Boltzmann function, the half-maximum activation voltage ($V_{1/2}$) and slope factor (k) were -25.9 ± 2.0 mV and 6.0 ± 0.3, respectively. The average current density measured with voltage steps to 0 mV, where HERG channels are fully activated, was 53.4 ± 6.5 pA/pF ($n = 10$ cells).

Nontransfected HEK 293 cells contain a small-amplitude background current that includes a time-dependent component. This is shown in Fig. 3 (see lower set of current traces

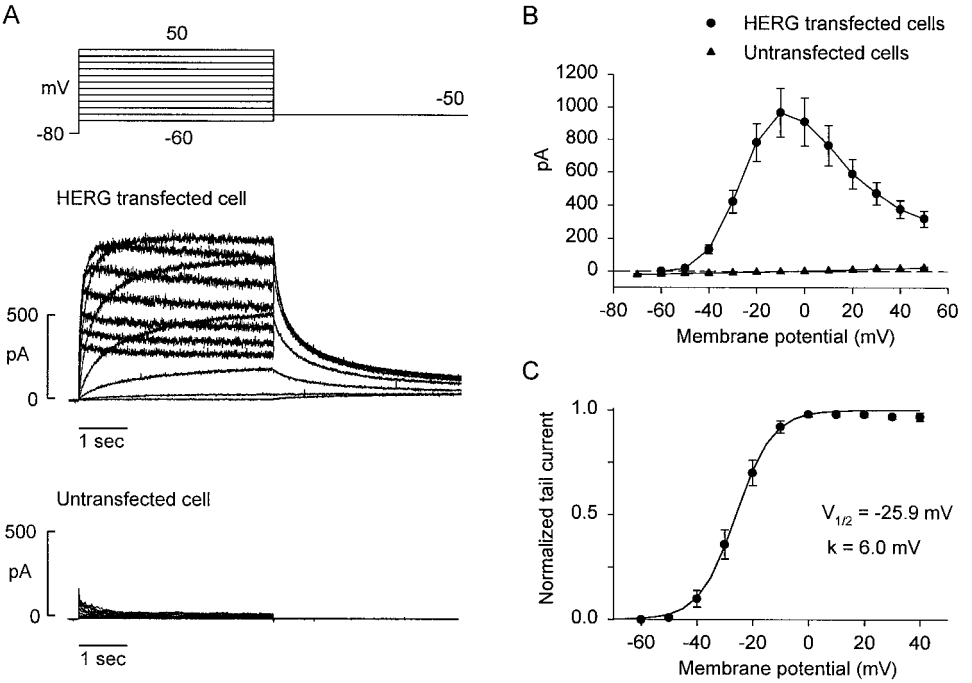

FIGURE 3 Electrophysiological properties of HERG current. (*A*) Voltage clamp protocol and currents recorded from a HERG-transfected cell (*upper set of current traces*) and an untransfected cell (*lower set of current traces*). Cells were held at −80 mV and depolarized to voltages between −60 and 50 mV for 4 s, and then clamped to −50 mV for 5 s. For the HERG-transfected cell, the peak outward current was reached with the depolarizing step to −10 mV. In the untransfected HEK 293 cell, a small-amplitude background current was present (see text). (*B*) *I-V* plot of HERG current (●, $n = 13$ cells) and the background current in untransfected cells (▲, $n = 6$) measured at the end of the depolarizing clamp steps. The dashed line indicates 0 current. (*C*) Activation curve measured with HERG tail currents and fitted to a Boltzmann relationship. The temperature was 35°C.

in Fig. 3 *A*). The voltage-clamp protocol is shown above. Depolarizing steps activated a small-amplitude outward current that decayed within several hundred milliseconds to a steady value. The peak current showed weak outward rectification consistent with the presence of a small-amplitude, endogenous current, and the current could be blocked by the application of 2 mM 4-AP (data not shown). The *I-V* plot of the current present at the end of the 4-s-long depolarizing steps showed a linear relation consistent with a small-amplitude leak current ($n = 6$ cells, Fig. 3 *B*, *triangles*). Electrophysiological properties of HERG-transfected HEK 293 cells compared with untransfected cells are summarized in Table 1.

The fully activated *I-V* plot for HERG-transfected cells is shown in Fig. 4. HERG current was activated by a depolarizing step to 60 mV for 1 s, and this was followed by repolarizing steps to different voltages, as shown in Fig. 4 *A*. At the more positive repolarizing voltages, HERG current showed inward rectification, and the current amplitude was relatively constant. With repolarizing steps to more negative voltages, HERG current recovered from inactivation to reach a peak value from which it underwent voltage-dependent decay. Fig. 4 *B* shows the *I-V* plot of the peak current during repolarization ($n = 4$ cells). The fully activated *I-V* plot shows inward rectification at more positive voltages, with maximum outward current obtained at voltages between −20 and −30 mV. Outward current was recorded to −85 mV, and at more negative voltages the current became inward.

TABLE 1 Electrophysiological properties of HERG-transfected HEK 293 cells

	HERG-transfected cells	Untransfected cells
Resting potential (mV)	−56 ± 1 ($n = 10$)	−11 ± 2 ($n = 11$)
Membrane capacitance (pF)	19.5 ± 1.2 ($n = 10$)	17.2 ± 0.8 ($n = 8$)
Input resistance (GΩ)	1.8 ± 0.1 ($n = 10$)	1.9 ± 0.3 ($n = 8$)
HERG current density (pA/pF)	53.4 ± 6.5 ($n = 10$)	—

Evidence confirming that the stably transfected HERG channel is selective for K^+ is shown in Fig. 5. Original current traces from one cell in different $[K^+]_o$ are shown in Fig. 5, *A–C*. From a holding potential of −80 mV, cells were depolarized to 20 mV for 0.5 s before being repolarized in 5-mV increments to different voltages bracketing the reversal potential. In Fig. 5 *A*, $[K^+]_o$ is 4 mM (the concentration normally used), and the reversal potential for tail current is close to −85 mV. In Fig. 5 *B*, $[K^+]_o$ is 2 mM and the reversal potential is close to −100 mV. In Fig. 5 *C*, $[K^+]_o$ is 10 mM and the reversal potential is close to −65 mV. Fig. 5 *D* shows summarized data of the dependence of reversal potential on $[K^+]_o$. In 2, 4, and 10 mM $[K^+]_o$, the reversal potentials were −97.9 ± 0.9 ($n = 6$ cells), −85.0 ± 0.9 ($n = 9$ cells), and −64.0 ± 0.8 ($n = 5$ cells) mV, respectively. When fit to a linear function, a slope value of 48.8 mV/10-fold change in $[K^+]_o$ was obtained. Using the Goldman-Hodgkin-Katz equation (Goldman, 1943; Hodgkin and Katz, 1949) to fit the data points and assuming K^+ and Na^+ to be the permeant ions gave a permeability ratio of Na^+/K^+ of 0.008 (Fig. 5 *D*, *solid line*). These data confirm high K^+ selectivity for the transfected HERG channel. The data in Fig. 5, *A–C*, also show that HERG current amplitude was increased at higher $[K^+]_o$, similar to that previously shown in oocytes for HERG (Sanguinetti et al., 1995) and in native heart cells for I_{Kr} (Sanguinetti and Jurkiewicz, 1990).

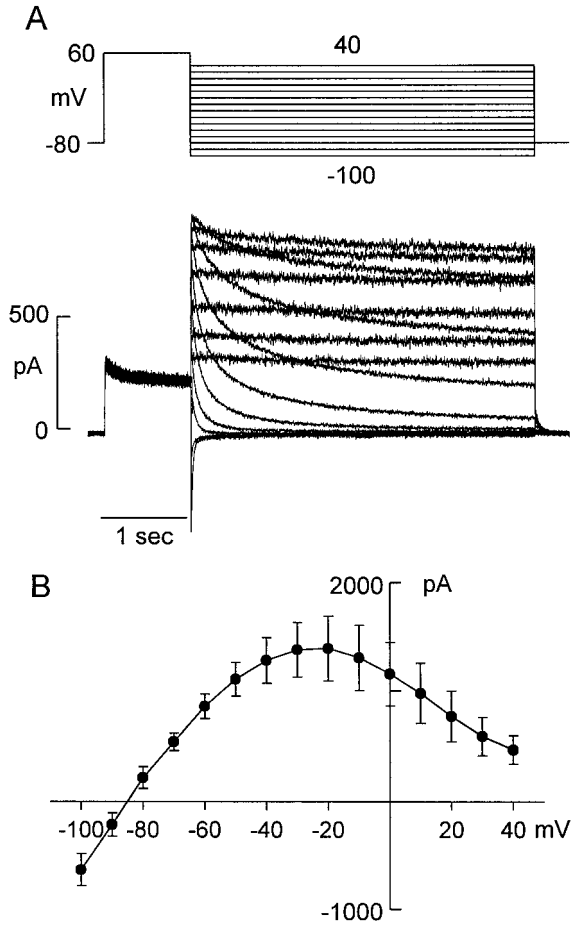

FIGURE 4 The fully activated *I-V* relation of HERG current. (*A*) Voltage clamp protocol and currents in a HERG-transfected cell. The cell was depolarized to 60 mV to activate and partially inactivate the HERG current. The cell was then repolarized to different voltages. With repolarization, current amplitude increased to reach a peak value at −20 mV in this cell. (*B*) *I-V* plot of the peak HERG current ($n = 4$ cells). For the fully activated *I-V* plot, the maximum current was obtained at voltages between −30 and −20 mV. The temperature was 35°C.

The time constants of HERG activation and deactivation are shown in Fig. 6. The activation time course between −40 and 60 mV was measured by two methods. The first method we used was to fit the rising phase of a current trace as a single exponential function (Sanguinetti et al., 1995; Snyders and Chaudhary, 1996). Original current traces are shown in Fig. 6 *A* (*upper panel*), and a single exponential fit to the current trace for the longest duration depolarizing step is shown on an expanded time scale in the lower panel. The initial current jump (80 pA) for the fit to a sustained depolarization is due to activation of the small-amplitude background currents (see Fig. 3). The second method was to fit the envelope of tail currents obtained from depolarizing steps applied for varying durations, followed by a repolarizing step to elicit tail current (Trudeau et al., 1995). Original tail current traces obtained with this method are also shown in Fig. 6 *A* (*upper panel*), and the peak tail current (*circles*) and single exponential fit (*solid line*) are shown in the lower panel. These two fitting approaches usually gave similar time constant values. At voltages above 0 mV, however, a single exponential fit to the rising phase of the current trace yielded a greater discrepancy compared with tail currents, most likely because of the development of rapid inactivation (Liu et al., 1996; Wang et al., 1997). For this reason, steps to voltages to ≥0 mV were fit by an envelope of tails method, whereas at more negative voltages, the simpler approach of fitting the rising phase of the current trace was used. The activation time constants are plotted in Fig. 6 *C*, summarized in Table 2, and were steeply voltage dependent. At 35°C and at more positive voltages, HERG activation is rapid. The HERG deactivation time course was obtained by fitting the decay of tail current as a double exponential function, and Fig. 6 *B* shows an example fit to HERG current at −70 mV after an initial depolarizing step to 60 mV for 1 s. Averaged data in Fig. 6 *C* also show the voltage dependence of the fast (τ_{Fast}) and slow (τ_{Slow}) time constants of deactivation of HERG current. Individual data values are summarized in Table 2. Table 2 also gives the relative amplitudes ($A_{Fast}/(A_{Fast} + A_{Slow})$) of the fast and slow current decays. The data show that both the fast and slow components of deactivation are steeply voltage dependent, and that the amplitude of the fast component is larger at more negative voltages, whereas the amplitude of the slow component becomes dominant at more positive deactivation voltages. These data agree with those of Snyders and Chaudhary (1996), who studied HERG current in transiently transfected HEK 293 cells, but are different from those of Sanguinetti et al. (1995; but see Sanguinetti et al., 1996a), who showed in oocytes that the amplitude of the fast component was smaller at more negative voltages and larger at more positive voltages.

The time courses of HERG current inactivation and recovery from inactivation are shown in Fig. 7. To measure the time constant of inactivation directly, we used a three-pulse protocol (Fig. 7 *A*; see also Smith et al., 1996; Spector et al., 1996b; Snyders and Chaudhary, 1996; Wang et al., 1997). In this protocol HERG current was activated and inactivated by 200-ms-long depolarizing steps to 60 mV. The cell was then repolarized to −100 mV for 2 ms to allow for recovery from inactivation (a time constant of 0.55 ms permits >95% recovery) without significant deactivation of HERG current (τ_{Fast} of 16 ms; see Table 2). The test step was applied to different voltages to observe the inactivation of HERG current. As shown in Fig. 7 *A*, the currents elicited by the test steps were of large amplitude and were rapidly inactivated. The time constant of inactivation was obtained by fitting the current with a single exponential function, and the averaged data are plotted in Fig. 7 *C* (*squares*, $n = 3$ cells). The time constant of recovery from inactivation was measured using a two-pulse protocol (Fig. 7 *B*; see also Spector et al., 1996b; Snyders and Chaudhary, 1996), in which the cell was depolarized to 60 mV for 200 ms to activate and inactivate HERG channels, and then was repolarized to voltages between −20 and −100 mV to give a tail current. This protocol generated the rapid recovery of

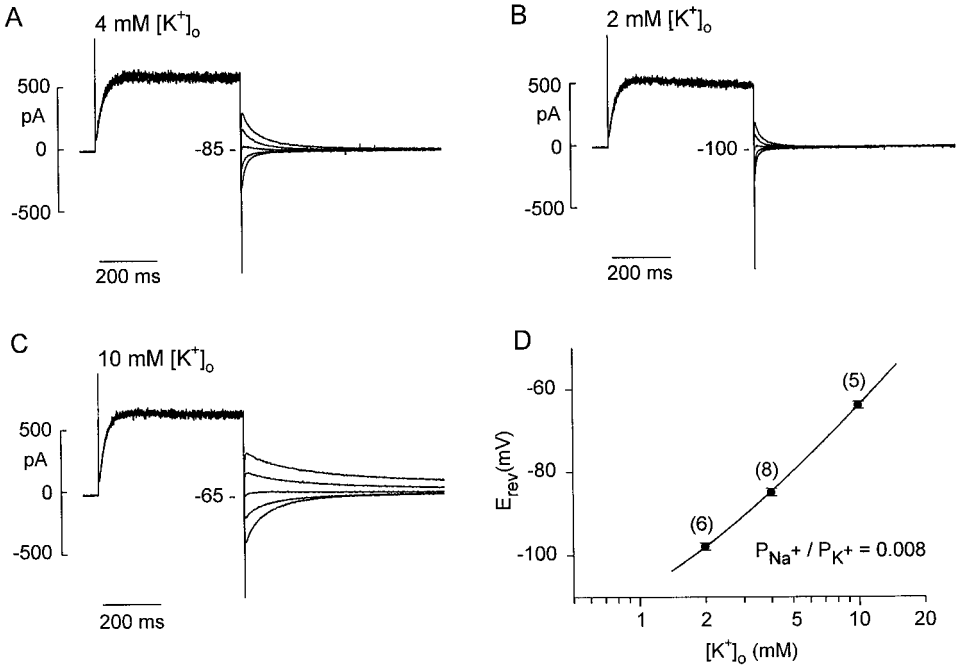

FIGURE 5 Dependence of HERG current on extracellular K^+. (*A–C*) Currents recorded from one cell in different $[K^+]_o$ with repolarizing steps in 5-mV increments to voltages bracketing the reversal potential. *A* shows currents for repolarizing steps to voltages between −75 and −95 mV. *B* shows currents for repolarizing steps to voltages between −90 and −110 mV. *C* shows currents for repolarizing steps to voltages between −55 and −75 mV. The reversal potential was measured in each cell as the zero intercept of the plot of tail current amplitude at each repolarizing voltage. (*D*) Average reversal potential plotted against log $[K^+]_o$, with the number of cells studied shown in parentheses. The line represents the fit of the data points to the GHK equation, $E_{rev} = 61.1 \times \log\{(p[Na^+]_o + [K^+]_o)/(p[Na^+]_I + [K^+]_I)\} + V_{off}$, where p is permeability and V_{off} is 4.9 mV (see Snyders et al., 1993). The temperature was 35°C.

HERG current, or a "hook." The time constant of recovery from inactivation was measured as the monoexponential fit to the tail current rising phase (> -40 mV) or as the fast time constant of a double-exponential fit (≤ -40 mV), where deactivation is present in the tail current. These data are plotted in Fig. 7 *C* (*circles*, $n = 3$ cells).

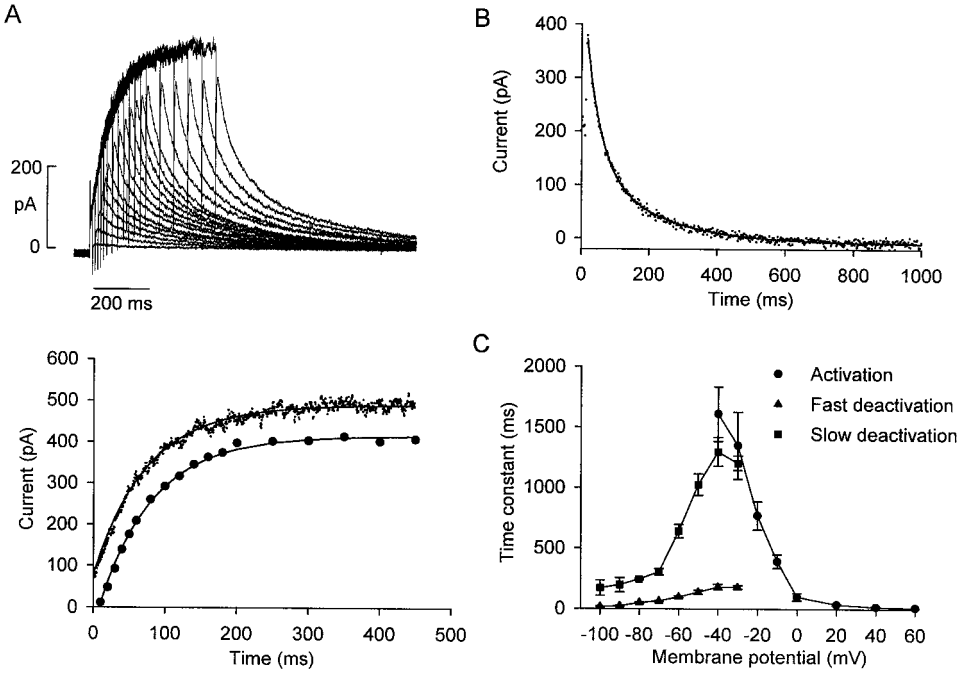

FIGURE 6 Time courses of HERG current activation and deactivation. Activation was measured by two methods, as shown in *A*. From the holding potential of −80 mV, the cell was clamped to 0 mV for different times before it was repolarized to −60 mV. As shown in the upper set of current traces, this permitted the recording of current during the depolarizing step and the recording of the envelope of tail current. The lower panel shows single exponential fits (*solid lines*) to both the maintained outward current (*continuous current trace*) and to the peak tail current envelope (*circles*). The time constants for activation were 77 and 78 ms, respectively. (*B*) Current decay in a different cell after stepping from 60 to −70 mV, and the double exponential fit to the data (*solid line*). The fast (τ_{Fast}) and slow (τ_{Slow}) time constants were 54 and 264 ms, respectively. (*C*) Voltage dependence of activation and fast and slow deactivation time constants. The temperature was 35°C.

TABLE 2 Voltage dependence of activation and deactivation of HERG

Activation (n = 4 or 5 cells at each voltage)								
Voltage (mV)	−40	−30	−20	−10	0	20	40	60
τ (ms)	1611 ± 225	1351 ± 277	770 ± 117	391 ± 57	98 ± 99	37 ± 5	18 ± 3	11 ± 1
Deactivation (n = 6 cells)								
Voltage (mV)	−100	−90	−80	−70	−60	−50	−40	−30
τ_{Fast} (ms)	16 ± 2	22 ± 4	50 ± 4	64 ± 5	97 ± 8	137 ± 16	180 ± 30	176 ± 27
τ_{Slow} (ms)	171 ± 63	196 ± 59	244 ± 6	303 ± 26	640 ± 56	1027 ± 89	1299 ± 118	1205 ± 59
$A_{Fast}/(A_{Fast} + A_{Slow})$	0.91 ± 0.02	0.87 ± 0.01	0.92 ± 0.01	0.81 ± 0.04	0.69 ± 0.03	0.54 ± 0.04	0.45 ± 0.04	0.39 ± 0.04

Effect of temperature on HERG current

Some experimental protocols were performed in the same cells at both 23°C and 35°C. Fig. 8 *A* shows an example of the effect of these temperatures on HERG current. The current was activated by a depolarizing step from −80 to 0 mV for 5 s, and tail current was recorded after a repolarizing step to −50 mV. With this voltage protocol, increasing the bath temperature from 23°C to 35°C resulted in several changes, including a marked increase in the amplitude of the outward and tail currents, and acceleration of the rates of activation, recovery from inactivation, and deactivation. In cells studied at both temperatures, the average current density measured at the end of the 5-s-long step to 0 mV was increased more than twofold from 21.7 ± 4.1 to 48.1 ± 9.5 pA/pF (n = 5 cells, $p < 0.05$). The time constant for current activation at 0 mV (obtained using the single exponential fitting procedure; see Fig. 6) was accelerated from 947 ± 87 to 105 ± 15 ms (n = 6 cells, $p < 0.05$). The deactivation of HERG current was fit by a double exponential function at both temperatures (see Fig. 6). The time constants of current deactivation at −50 mV were decreased from 216 ± 19 to 149 ± 27 ms for τ_{Fast} and from 1425 ± 213 to 1086 ± 136 ms for τ_{Slow} (n = 3 cells, $p < 0.05$). With the three-pulse protocol shown in Fig. 7 *A* (repolarizing step durations to −100 mV of 10 and 2 ms at 23°C and 35°C, respectively) to measure inactivation, or the two-pulse protocol in Fig. 7 *B* to measure recovery from inactivation, increasing temperature from 23°C to 35°C markedly accelerated these time courses. The time constant of inactivation at 0 mV was decreased from 14.2 ± 1.3 ms to 3.1 ± 0.3 ms (n = 3 cells, $p < 0.05$), and the time constant of recovery from inactivation at −50 mV was decreased from 8.5 ± 0.6 ms to 1.8 ± 0.1 ms (n = 3 cells, $p < 0.05$). Finally, as shown in Fig. 8 *B*, increasing temperature from 23°C to 35°C shifted

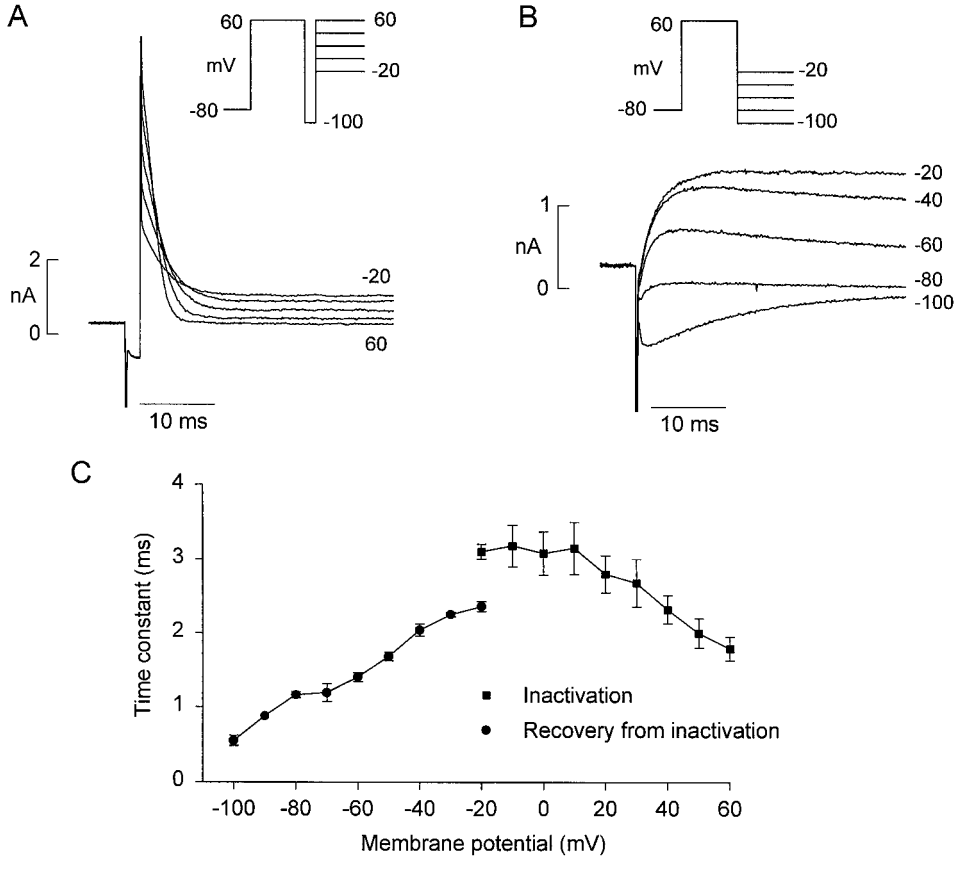

FIGURE 7 Inactivation and recovery from inactivation. (*A, inset*) Three-pulse protocol used to study inactivation properties of HERG current. The HERG current traces surrounding the repolarizing step to −100 mV are shown on an expanded time scale. (*B, inset*) Protocol used to study recovery from inactivation. The current traces following the steps to different voltages are shown on an expanded time scale. (*C*) Voltage dependence of the time constants for the development of inactivation (■) and recovery from inactivation (●). The temperature was 35°C.

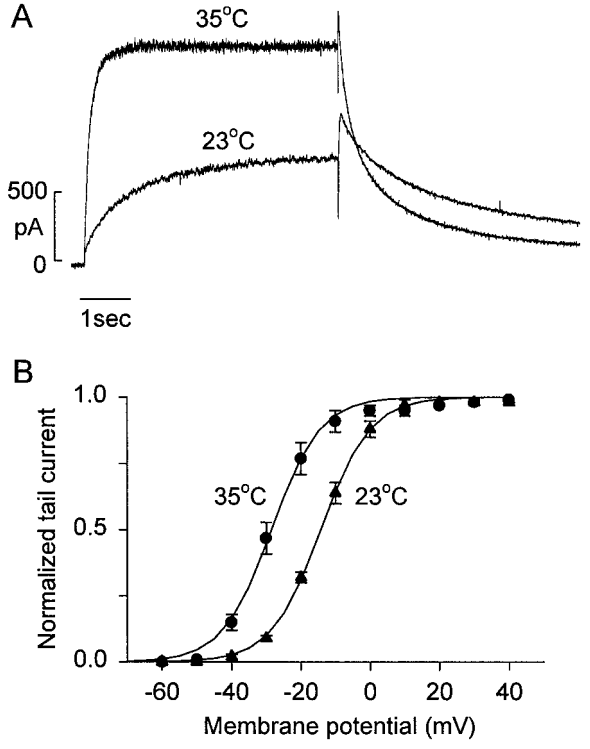

FIGURE 8 Temperature dependence of HERG current. (*A*) Current traces recorded from a stably transfected HEK 293 cell at 23°C and 30 s later at 35°C. The cell was held at −80 mV and clamped to 0 mV for 5 s, and tail current was recorded with a repolarizing step to −50 mV. (*B*) Activation curve (voltage clamp protocol is the same as that used in Fig. 3) obtained in four cells studied at both temperatures.

the activation curve negatively ($V_{1/2}$ from −14.2 ± 1.1 mV to −28.1 ± 1.8 mV, $p < 0.05$), with no change in the slope factor (from 7.13 ± 0.43 to 7.05 ± 0.86, $n = 4$ cells, $p > 0.05$).

Low concentrations of E-4031 block HERG current

The sensitivity of transfected HERG channels to the methanesulfonanilide drug E-4031 was studied because previous reports in oocytes have suggested that E-4031 block of HERG channels requires high drug concentrations (Trudeau et al., 1995; Spector et al., 1996a). In the experiments shown in Fig. 9, HERG current was activated by a 4-s-long depolarizing pulse to 0 mV from a holding potential of −80 mV, and the tail current was recorded at −50 mV. After control currents were recorded, the cell was held continuously at the holding potential of −80 mV during drug wash-in to maintain channels in a closed state. As shown in the upper left current traces, after a 10-min drug wash-in period of 30 nM E-4031, HERG current amplitude activated with the first depolarizing step was initially changed little from the control current, suggesting minimal drug binding to closed channels. However, during the depolarizing step, current amplitude gradually declined as drug block accumulated. Depolarizing steps were applied at 15-s intervals, and with each subsequent depolarizing step drug block of HERG channels increased until a steady-state level of block was reached by the 10th to 12th depolarizing steps. Fig. 9 also shows the results from a different cell exposed to 300 nM E-4031 (*upper right current traces*). Control current was recorded with a depolarizing step from −80 to 0 mV. After a 10-min-long drug wash-in period of 300 nM E-4031, the initial amplitude of the HERG current activated with the first depolarizing step was only minimally reduced from the control current level. However, during the depolarizing step, current amplitude rapidly decreased as drug block developed. The current was completely blocked at the end of the second depolarizing step. Recovery from block between depolarizing steps was minimal with this protocol. Fig. 9 shows the concentration dependence of steady-state block of HERG tail current by E-4031 compared with the control value. The dose-response curve for E-4031 block showed an IC_{50} of 7.7 nM and a Hill coefficient of 1.0. At an E-4031 concentration of 300 nM, steady-state drug block left only the small background outward current (see also Fig. 10). Washout of E-4031 resulted in the partial recovery of HERG current within 10–20 min (data not shown).

HERG current during cardiac action potential clamp

The potential contribution of HERG current during a cardiac action potential was studied using an action potential clamp method, as shown in Fig. 10. Fig. 10 *A* (*upper trace*) shows an action potential waveform recorded from a rabbit ventricular myocyte (Zhou et al., 1995), which was used as the command voltage to clamp HERG transfected cells. The currents recorded during an action potential clamp under control conditions and in the presence of steady-state block with 300 nM E-4031 are shown in the lower traces in Fig. 10 *A*. HERG current is expressed as the E-4031-sensitive current, and it shows that HERG current activates rapidly, reaching an initial peak value within 21 ms (*point a*) in this cell. After a small decay in current amplitude, presumably due to channel inactivation, the current then increased progressively to reach a maximum at −30 mV (*point b*) as the action potential repolarized. Fig. 10 *B* shows the instantaneous *I-V* relation derived by plotting against each other the action potential clamp voltage and E-4031-sensitive current traces in Fig. 10 *A*. It demonstrates that HERG contributes current throughout the action potential, but the HERG current is largest during phases 2 and 3 (the plateau and terminal repolarization phases) of the action potential. To confirm that HERG current can repolarize a cell, we switched from voltage clamp to zero-current clamp mode during repolarization. As shown in Fig. 10 *C*, an action potential waveform was applied as the command voltage. The cell was then released from voltage clamp, which resulted in the rapid repolarization of the membrane potential to −85 mV, the reversal potential for HERG current in 4 mM $[K^+]_o$. After reaching the reversal potential, the membrane then gradually depolarized to ~ −50 mV, which

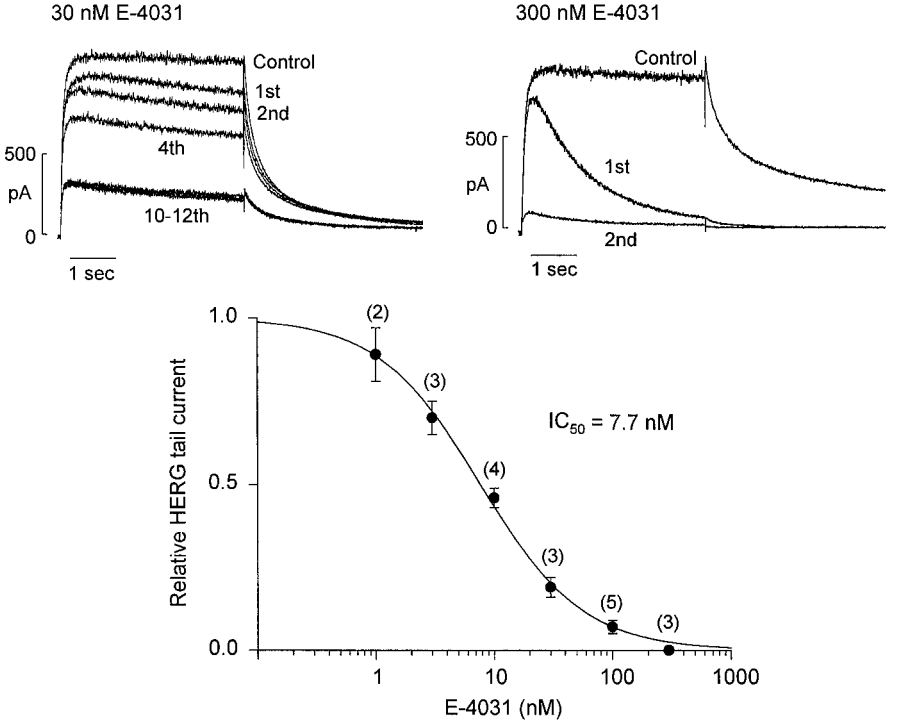

FIGURE 9 Block of HERG current by E-4031. Left-hand current traces show the effect of 30 nM E-4031. Steady-state block was reached by the 10th to 12th depolarizing steps. With 300 nM E-4031 (*upper right-hand current traces*) drug block was nearly complete by the end of the second depolarizing step. The steady-state dose-response relation for E-4031 (*the number of cells is given in parentheses*). The IC_{50} for E-4031 drug block was 7.7 nM. The temperature was 35°C.

is close to the resting potential in HERG-transfected HEK 293 cells.

DISCUSSION

An important aspect of this work is the development of stable cell lines expressing high levels of functional HERG channels. The HEK 293 cells are easily studied, and we used these cells to investigate biochemical properties of HERG protein, and to study electrophysiological and pharmacological properties of HERG channels at physiological temperatures.

Biochemical data

Using antibodies directed to the C- or N-terminus, two HERG protein bands were detected in the Western analysis

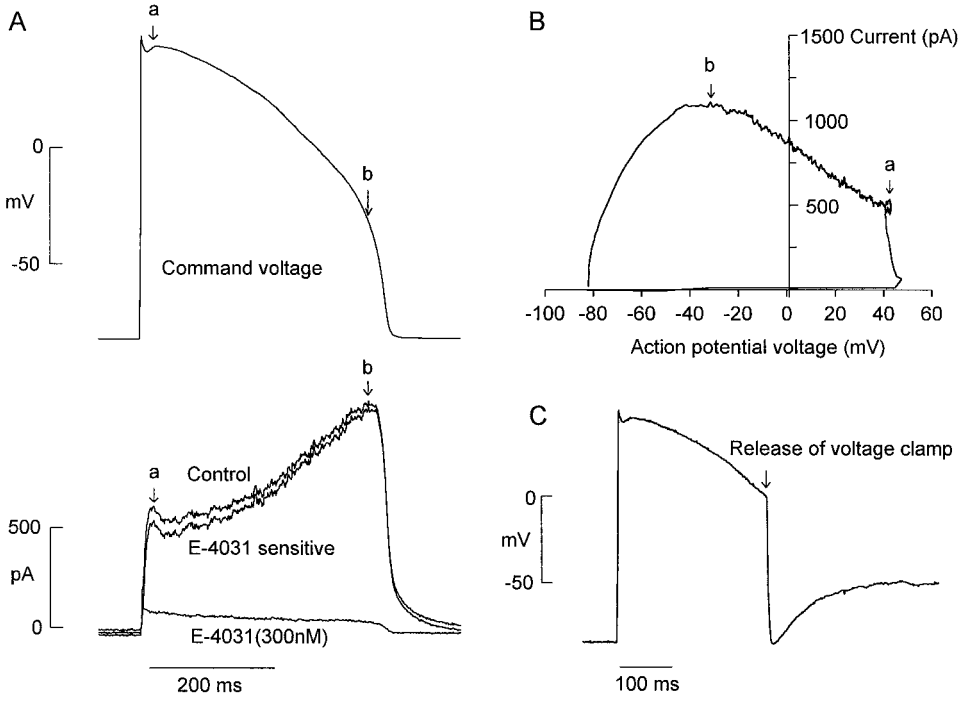

FIGURE 10 HERG current during a cardiac action potential clamp. (*A*) A ventricular action potential voltage clamp waveform (*upper trace*) applied to the cell to activate HERG current (*lower trace*). HERG current, shown as the E-4031-sensitive current (control current − residual current in 300 nM E-4031), begins to activate rapidly to reach an initial peak value in 21 ms (*point a*). After a small decay in amplitude, HERG current increased progressively as the action potential repolarized to reach a second peak (*point b*). The instantaneous *I-V* relation during the action potential clamp (*B*) (E-4031-sensitive current) shows that HERG contributes repolarizing current broadly throughout the action potential, and that it is maximum at voltages close to −30 mV. (*C*) A release from the voltage clamp protocol, where the membrane repolarized to the reversal potential and then gradually depolarized as HERG channels deactivated. The temperature was 35°C.

in HERG-transfected HEK 293 cells. Both bands are larger than the predicted molecular mass of 127 kDa from the deduced amino acid sequence of HERG protein (Warmke and Ganetzky, 1994). This suggests that the smaller band is not a degradation product. Many channel proteins show more than one band on Western blot analyses (for examples, see Deal et al., 1994; Santacruz-Toloza et al., 1994; Krapivinsky et al., 1995), which is often attributed to glycosylation of the channel protein in the endoplasmic reticulum and Golgi apparatus. For Shaker K^+ channels, the fully glycosylated protein is thought to be the mature form of the channel, and the core-glycosylated protein, which gives a smaller molecular mass protein, is the precursor form of the channel (Santacruz-Toloza et al., 1994). The HERG protein sequence contains six consensus sites for *N*-glycosylation (Warmke and Ganetzky, 1994). Two of these sites are located extracellularly, as derived from proposed models of membrane topology for the HERG channel. One site (N598) is located 14 amino acids upstream of the pore region, and the other (N629) is located within the pore region. Further studies are needed to elucidate whether one or both of these sites are glycosylated.

The finding that *N*-glycosidase F treatment did not convert both proteins to a single band suggests that posttranslational modification other than N-linked glycosylation may also be involved. These modifications may involve *O*-glycosylation, phosphorylation, palmitylation, sulfation, or acylation, as reported in sodium channels (Schmidt and Catterall, 1987) and Kv1.1 channels (Deal et al., 1994). Another possibility is incomplete digestion of the carbohydrate by *N*-glycosidase F treatment.

HERG at physiological temperatures: comparison with I_{Kr}

Previously reported experiments studied HERG channel current expressed in oocytes or transiently in HEK 293 cells and were performed at room temperature (Sanguinetti et al., 1995; Trudeau et al., 1995; Snyders and Chaudhary, 1996; Wang et al., 1997). At 23°C, the kinetic values we found for HERG channel current stably transfected in HEK 293 cells were similar to previously reported values. More importantly, our data show that the kinetic properties measured for HERG current are markedly dependent on temperature. At 35°C, current amplitude was increased by more than twofold, and kinetic properties were accelerated. It is interesting that the greatest temperature effect was on the rate of current activation, followed by the rates of inactivation and recovery from inactivation, and with the least effect on the rate of deactivation. These findings should account, at least in part, for the marked increase in HERG current amplitude at 35°C. Clearly, the temperature dependence of the kinetic steps underlying HERG channel gating is complex.

It is important to compare our results with findings reported for I_{Kr}. For activation, the most detailed data for human I_{Kr} were obtained by Wang et al. (1994) in atrial cells. They showed that at 36°C the E-4031-sensitive current activation had voltage and time dependence similar to our findings obtained with HERG expressed in HEK 293 cells and studied at 35°C. Veldkamp and co-workers (1995) studied I_{Kr} in human ventricular cells and reported at 30 mV a mean activation time constant of 101 ms. In myocytes from some species studied at physiological temperatures (guinea pig ventricular cells, see Sanguinetti and Jurkiewicz, 1990; canine ventricular cells, see Liu and Antzelovitch, 1995), the time and voltage dependences of I_{Kr} activation are also close to what we found with HERG, although in other species slower activation kinetics values have been reported (rabbit ventricular cells; Clay et al., 1995). We conclude that differences in activation kinetic properties between HERG current and I_{Kr}, a concern in several previous reports, are diminished when studies are performed at physiological temperatures.

Inactivation and recovery from inactivation of I_{Kr} has been studied in ferret atrial cells at room temperature (Liu et al., 1996). Using voltage protocols similar to ours, these investigators report time constants for the development of inactivation and recovery from inactivation that are comparable to our data obtained with HERG current at 23°C. Similar findings have also been reported for I_{Kr} in mouse atrial tumor (AT-1) cells (Yang et al., 1997).

For deactivation of I_{Kr}, few data are available for comparison. In human atrial myocytes, deactivation of an E-4031-sensitive current component at −40 mV had a time constant of 234 ms when fit with a single exponential function (36°C; Wang et al., 1994). This value is similar to the fast deactivation time constant we obtained at this voltage (see also Sanguinetti and Jurkiewicz, 1990). By using a double exponential fitting technique, deactivation fast and slow time constants have been obtained in canine ventricular cells (36°C; Liu and Antzelovitch, 1995) and in AT-1 cells (22–23°C; Yang et al., 1994). In the canine cells, the fast and slow time constants were somewhat slower than the values we obtained, whereas for the mouse AT-1 cells, a striking finding is that both the fast and slow components of I_{Kr}, even at the lower temperature, deactivated more rapidly than HERG current in our HEK 293 cells. The explanation for these apparent kinetic differences is not clear, although one possibility is that structural differences exist between HERG channels expressed in HEK 293 cells and mouse AT-1 cell I_{Kr} channels. Recent findings of a HERG cardiac-specific isoform in mouse with faster deactivation kinetics support this hypothesis (London et al., 1997).

E-4031 binding to HERG channels

E-4031, a methanesulfonanilide antiarrhythmic drug prototype having a class III (QT prolonging) effect, is thought in cardiac cells to block I_{Kr} with high selectivity. In native guinea pig cells, E-4031 originally was reported to block I_{Kr} with an IC_{50} of 397 nM (Sanguinetti and Jurkiewicz, 1990). Subsequent reports, however, found greater drug sensitivity

for E-4031 block of I_{Kr} in ferret atrial myocytes (IC_{50} 10.3 nM; Liu et al., 1996) and in preliminary experiments in rabbit ventricular myocytes (IC_{50} ~20 nM; Zhou et al., 1995). In the present experiments in HEK 293 cells, we found that E-4031 blocked HERG current in similarly low concentrations (IC_{50} 7.7 nM). Our results are different from those obtained in oocyte expression systems where HERG current is sensitive to E-4031, but with a higher IC_{50} of 588 nM (Trudeau et al., 1995; see also Spector et al., 1996a). The differences between the IC_{50} values reported for block of HERG current expressed in oocytes verses our HEK 293 cells or for I_{Kr} in native heart cells is uncertain, but may be attributed to experimental technique and protocol differences, the effects of restricted drug diffusion at the surface membrane and yolk sac absorption in oocytes, and as well possible structural differences between HERG and I_{Kr} in different mammalian heart cells. It is interesting that dofetilide, another methanesulfonanilide drug, also blocks with high-affinity HERG current in transiently transfected HEK 293 cells (IC_{50} 12.6 nM; Snyders and Chaudhary, 1996) and blocks with reduced affinity HERG current expressed in intact oocytes (IC_{50} 595 nM; Kiehn et al., 1996). With the use of inside-out macropatches from oocytes, however, higher affinity dofetilide block of HERG current has been obtained (IC_{50} 35 nM, Kiehn et al., 1996). Our data show high E-4031 drug sensitivity close to that found for I_{Kr} in native heart cells, and suggest that the stably transfected cells we used are likely to be preferable to oocyte expression systems as an experimental model for pharmacological studies.

Our results also show that E-4031 does not block closed channels. Even at high concentrations (300 nM), E-4031 drug binding to closed states was minimal. Rather, drug block of HERG current required channel activation consistent with activated block, and our results agree with previous findings (see Trudeau et al., 1995; Spector et al., 1996a; Snyders and Chaudhary, 1996). Our protocols, however, do not distinguish between open or inactivated channel block.

HERG current during cardiac action potentials

HERG current, or I_{Kr}, is thought to contribute to the repolarization of the cardiac action potential. Our results with the action potential clamp method show this directly. At 35°C action potential, depolarization rapidly activates HERG channels, and they begin to contribute repolarizing current shortly after the action potential reaches its peak voltage. HERG current reaches an initial peak value from which it declines, presumably because of voltage-dependent inactivation which is rapid at more positive voltages and limits the amount of time channels spend in an open state. More importantly, as repolarization progresses, HERG current gradually increases as channels rapidly recover from inactivation. Thus critical determinants of the current profile during repolarization of the action potential are the rate of recovery from inactivation and the rate of deactivation. This is in contrast to other K^+ channels, the physiological roles of which are generally attributed to their rates of activation and inactivation during depolarization. The increase in HERG current during repolarization encompasses a broad voltage range, and it reaches a maximum during phases 2 and 3 of the cardiac action potential. Because HERG current amplitude is largest at these voltages, drug block or molecular defects that reduce HERG current (causing long QT syndrome) will be expected to exert their greatest action potential prolonging effects in these regions of the action potential. This also provides insight into why suppression of I_{Kr} in native heart cells leads to the induction of early after-depolarizations arising from action potential plateau voltages (see January and Zhou, 1997).

Finally, HERG deactivates with a time- and voltage-dependent delay (see Fig. 6 and Table 2). As shown in Fig. 10, HERG continues to contribute current throughout the return of the membrane to the resting potential and into the post-repolarization interval. Thus, as a deactivating K^+ current, HERG channels could serve as a pacemaking mechanism contributing to phase 4 depolarization. The release from voltage clamp experiment shown in Fig. 10 *C*, although performed in a transfected cell, clearly demonstrates the potential pacemaking properties of HERG. A role in pacemaking for an E-4031-sensitive, delayed rectifier K^+ current has been proposed for SA node cells (see Verheijck et al., 1995, for discussion).

The authors thank Drs. A. Pond and J. Nerbonne, Department of Pharmacology and Molecular Biology, Washington University (St. Louis, MO), for the anti-HERG antibodies.

REFERENCES

Clay, J. R., A. Ogbaghebriel, T. Paquette, B. I. Sasyniuk, and A Shrier. 1995. A quantitative description of the E-4031 sensitive repolarization current in rabbit ventricular myocytes. *Biophys. J.* 69:1830–1837.

Curran, M. E., I. Splawski, K. W. Timothy, G. M. Vincent, E. D. Green, and M. T. Keating. 1995. A molecular basis for cardiac arrhythmia: HERG mutations cause long QT syndrome. *Cell.* 80:795–803.

Deal, K. K., D. M. Lovinger, and M. M. Tamkun. 1994. The brain Kv1.1 potassium channel: in vitro and in vivo studies on subunit assembly and posttranslational processing. *J. Neurosci.* 14:1666–1676.

Goldman, D. E. 1943. Potential, impedance and rectification in membranes. *J. Gen. Physiol.* 27:37–60.

Hamill, O. P., A. Marty, E. Neher, B. Sakmann, and F. J. Sigworth. 1981. Improved patch-clamp techniques for high resolution current recording from cells and cell-free membrane patches. *Pflugers Arch.* 391:85–100.

Hodgkin, A. L., and B. Katz. 1949. The effect of sodium ions on the electrical activity of the giant axon of the squid. *J. Physiol. (Lond.).* 108:37–77.

January, C. T., and Z. Zhou. 1997. Early afterdepolarizations: mechanisms and possible role in arrhythmias. *In* Electrocardiology '96: From the Cell to the Body Surface. J. Liebman, editor. World Scientific, Singapore. 231–240.

Kiehn, J., A. E. Lacerda, B. Wible, and A. M. Brown. 1996. Molecular physiology and pharmacology of HERG: single-channel currents and block by dofetilide. *Circulation.* 94:2572–2579.

Krapivinsky, G., E. A. Gordon, K. Wickman, B. Velimirovic, L. Krapivinsky, and D. E. Clapham. 1995. The G-protein-gated atrial K^+ channel I_{KACh} is a heteromultimer of two inwardly rectifing K^+-channel proteins. *Nature.* 374:135–141.

Laemmli, U. K. 1970. Cleavage of structural proteins during the assembly of the head of bacteriophage T4. *Nature.* 227:680–685.

Li, G. R., J. Feng, Z. Wang, B. Fermini, and S. Nattel. 1996a. Adrenergic modulation of ultrarapid delayed rectifier K+ current in human atrial myocytes. *Circ. Res.* 78:903–915.

Li, G. R., J. Feng, L. Yue, M. Carrier, and S. Nattel. 1996b. Evidence for two components of delayed rectifier K^+ current in human ventricular myocytes. *Circ. Res.* 78:689–696.

Liu, D.-W., and C. Antzelovitch. 1995. Characteristics of the delayed rectifier current (I_{Kr} and I_{Ks}) in canine ventricular epicardial, midmyocardial, and endocardial myocytes. *Circ. Res.* 76:351–365.

Liu, S., R. L. Rasmusson, D. L. Campbell, S. Wang, and H. C. Strauss. 1996. Activation and inactivation kinetics of an E-4031-sensitive current from single ferret atrial myocytes. *Biophys. J.* 70:2704–2715.

London, B., M. C. Trudeau, K. P. Newton, A. K. Beyer, N. G. Copeland, D. J. Gilbert, N. A. Jenkins, C. A. Satler, and G. A. Robertson. 1997. Two isoforms of the mouse ether-a-go-go-related gene coassemble to form channels with properties similar to the cardiac current I_{Kr}. *Circ. Res.* (in press).

Maniatis, T., E. F. Fritsch, and J. Sambrook. 1987. Molecular Cloning. A Laboratory Manual. Cold Spring Harbor Laboratory, Cold Spring Harbor, NY.

Mohammad, S., Z. Zhou, Q. Gong, and C. T. January. 1997. Blockage of the HERG human cardiac K^+ channel by the gastrointestinal prokinetic agent cisapride. *Am. J. Physiol. (Heart Circ.).* 42:H2534–H2538.

Pond, A., and J. M. Nerbonne. 1996. A truncated form of HERG identified in human heart. *Circulation.* 94:I-641 (Abstr.).

Sanguinetti, M. C., M. E. Curran, P. S. Spector, and M. T. Keating. 1996a. Spectrum of HERG K+-channel dysfunction in an inherited cardiac arrhythmia. *Proc. Natl. Acad. Sci. USA.* 93:2208–2212.

Sanguinetti, M. C., M. E. Curran, A. Zou, J. Shen, P. S. Spector, D. L. Atkinson, and M. T. Keating. 1996b. Coassembly of KvLQT1 and minK (IsK) proteins to form cardiac I_{Ks} potassium channel. *Nature.* 384: 80–83.

Sanguinetti, M. C., C. Jiang, M. E. Curran, and M. T. Keating. 1995. A mechanistic link between an inherited and an acquired cardiac arrhythmia: HERG encodes the I_{Kr} potassium channel. *Cell.* 81: 299–307.

Sanguinetti, M. C., and N. K. Jurkiewicz. 1990. Two components of cardiac delayed rectifier K^+ current. *J. Gen. Physiol.* 96:195–215.

Santacruz-Toloza, L., Y. Huang, S. A. John, and D. M. Papazian. 1994. Glycosylation of Shaker potassium channel protein in insect cell culture and in Xenopus oocytes. *Biochemistry.* 33:5607–5613.

Schmidt, J. W., and W. A. Catterall. 1987. Palmitylation, sulfation, and glycosylation of the alpha subunit of the sodium channel. Role of post-translational modifications in channel assembly. *J. Biol. Chem.* 262:13713–13723.

Smith, P. L., T. Baukrowitz, and G. Yellen. 1996. The inward rectification mechanism of the HERG cardiac potassium channel. *Nature.* 379: 833–836.

Snyders, D. J., and A. Chaudhary. 1996. High affinity open channel block by dofetilide of HERG expressed in a human cell line. *Mol. Pharmacol.* 49:949–955.

Snyders, D. J., M. M. Tamkun, and P. B. Bennett. 1993. A rapidly activating and slowly inactivating potassium channels cloned from human heart: functional analysis after stable mammalian cell culture expression. *J. Gen. Physiol.* 101:513–543.

Spector, P., M. E. Curran, M. T. Keating, and M. C. Sanquinetti. 1996a. Class III antiarrhythmic drugs block HERG, a human cardiac delayed rectifier K^+ channel. *Circ. Res.* 78:499–503.

Spector, P., M. E. Curran, A. Zou, M. T. Keating, and M. C. Sanquinetti. 1996b. Fast inactivation causes rectification of the I_{Kr} channel. *J. Gen. Physiol.* 107:611–619.

Tanaka, T., R. Nagai, H. Tomoike, S. Takata, K. Yano, K. Yabuta, N. Haneda, O. Nakano, A. Shibata, T. Sawayama, H. Kasai, Y. Yazaki, and Y. Nakamura. 1997. Four novel KVLQT1 and four novel HERG mutations in familial long-QT syndrome. *Circulation.* 95:565–567.

Trudeau, M. C., J. W. Warmke, B. Ganetzky, and G. A. Robertson. 1995. HERG, a human inward rectifier in the voltage-gated potassium channel family. *Science.* 269:92–95.

Trudeau, M. C., J. W. Warmke, B. Ganetzky, and G. A. Robertson. 1996. HERG sequence correction [letter]. *Science.* 272:1087.

Veldkamp, M. W., A. G. C. van Ginneken, T. Opthof, and L. N. Bouman. 1995. Delayed rectifier channels in human ventricular myocytes. *Circulation.* 92:3497–3504.

Verheijck, E. E., A. C. G. van Ginneken, J. Bourier, and L. N. Bouman. 1995. Effects of delayed rectifier current blockade by E-4031 on impulse generation in single sinoatrial nodal myocytes of the rabbit. *Circ. Res.* 76:607–615.

Wang, S., S. Liu, M. J. Morales, H. C. Strauss, and R. L. Rassmusson. 1997. A quantitative analysis of activation and inactivation of HERG expressed in Xenopus oocytes. *J. Physiol. (Lond.).* 502:45–60.

Wang, Z., B. Fermini, and S. Nattel. 1993. Sustained depolarization-induced outward current in human atrial myocytes. Evidence for a novel delayed rectifier K^+ current similar to Kv1.5 cloned channel currents. *Circ. Res.* 73:1061–1076.

Wang, Z., B. Fermini, and S. Nattel. 1994. Rapid and slow components of delayed rectifier current in human atrial myocytes. *Cardiovasc. Res.* 28:1540–1546.

Warmke, J. W., and B. Ganetzky. 1994. A family of potassium channel genes related to *eag* in *Drosophila* and mammals. *Proc. Natl. Acad. Sci. USA.* 91:3438–3442.

Yang, T., D. J. Snyders, and D. M. Roden. 1997. Rapid inactivation determines the rectification and $[K^+]_o$ dependence of the rapid component of the delayed rectifier K^+ current in cardiac cells. *Circ Res.* 80:782–789.

Yang, T., M. S. Wathen, A. Felipe, M. M. Tamkun, D. J. Snyders, and D. M. Roden. 1994. K^+ currents and K^+ channel mRNA in cultured atrial cardiac myocytes (AT-1 cells). *Circ. Res.* 75:870–878.

Zhou, Z., Q. Gong, B. Ye, Z. Fan, J. C. Makielski, G. A. Robertson, and C. T. January. 1997. Electrophysiological and pharmacological properties of HERG channels in a stably transfected human cell line. *Biophys. J.* 72:A225 (Abstr.).

Zhou, Z., C. Studenik, and C. T. January. 1995. Mechanisms of early afterdepolarizations induced by block of I_{Kr}. *Circulation.* 92:I-435 (Abstr.).